Journal of Statistical Physics, Vol. 87, Nos. 3/4, 1997

On the Shape of Wedding Cakes

Joachim Krug[1]

Received August 27, 1996

The large-scale morphology of a growing surface is characterized for a simple model of crystal growth in which interlayer transport is completely suppressed due to the Ehrlich–Schwoebel effect. In the limit where the ratio of the surface diffusion coefficient to the deposition rate $D/F \to \infty$ the surface consists of wedding-cake-like structures whose shape is given by the inverse of an error function. The shape can be viewed as a separable solution of the singular diffusion equation $u_t = [u^{-2}u_x]_x$. As an application, expressions for the number of exposed layers as a function of coverage and diffusion length are derived.

KEY WORDS: Crystal growth; growth instability; surface diffusion; singular diffusion equations; hydrodynamic limit.

1. INTRODUCTION

The wedding cake morphology is a common occurrence in the low-temperature epitaxial growth of metal surfaces[1-3] (see ref. 4 for review). Microscopically it originates from an excess energy barrier at step edges, which prevents atoms from descending from the atomic layer on which they have been deposited.[5] As a consequence the concentration of adsorbed atoms (*adatoms*) on top of two-dimensional islands is increased, such that second-layer nucleation occurs well before the first-layer has been completed. This process repeats itself in subsequent layers, giving rise to a wedding-cake-like structure of islands on top of islands.

In the present paper I describe the asymptotic, large-scale shape of these structures within a minimal one-dimensional growth model[6] in which interlayer transport is completely inhibited. For this limiting case the layer coverages are known to follow a Poisson distribution.[7] Together with a few plausible simplifying assumptions, this turns out to be sufficient

[1] Fachbereich Physik, Universität GH Essen, D-45117 Essen, Germany.

0022-4715/97/0500-0505$12.50/0 © 1997 Plenum Publishing Corporation

to deduce the shape. Alternatively, the shape can be obtained as a separable solution of a singular diffusion equation, which has been studied previously in a variety of contexts.[8-11]

The growth model and its basic phenomenology is introduced in Section 2. Section 3 shows how the coverage distribution translates into the shape. A derivation of the continuum limit for the growth process is given in Section 4, and the relation to singular diffusion is discussed. Finally, Section 5 contains some results for two-dimensional surfaces.

2. MODEL AND PHENOMENOLOGY

Consider the one-dimensional integer lattice of sites x, with an integer height variable h_x defining the position of the surface above x. The model allows for two processes:[6] At rate F atoms are deposited at a randomly chosen position ($h_x \to h_x + 1$), and at rate D singly bonded adatoms hop to neighboring sites ($h_x \to h_x - 1$, $h_y \to h_y + 1$, $y = x \pm 1$), *provided* they remain within the same layer ($h_y = h_x - 1$ prior to the move). Atoms with more than one nearest neighbor bond (that is, with at least one horizontal bond) are immobile.

Since the time t will usually be measured in units of the coverage

$$\theta = Ft \tag{1}$$

the only model parameter is the ratio D/F; the interest is in the case $D/F \gg 1$, where long-ranged lateral correlations can develop. Figure 1 illustrates the time evolution, starting from a flat substrate ($h_x \equiv 0$), for $D/F = 5 \times 10^6$. Initially a freshly landed atom diffuses over the substrate until it encounters a second atom with which it forms an immobile dimer. The dimers act as nucleation centers for islands, which set the scale for the subsequent morphological evolution. Scaling arguments[12] and simulations[6, 12] show that the spacing L between first-layer islands is of the order

$$L \sim (D/F)^{1/4} \tag{2}$$

in one dimension.

Figure 1 indicates that the positions of the first-layer nucleation events essentially fix the positions of the peaks of the wedding cakes at all later times. This is because, after the deposition of a few layers, the peaks typically consist of towers one or at most two columns wide, which forces the nucleation of the next layer to occur at the same lateral position as in the layer below. In other words, due to the suppression of interlayer transport,

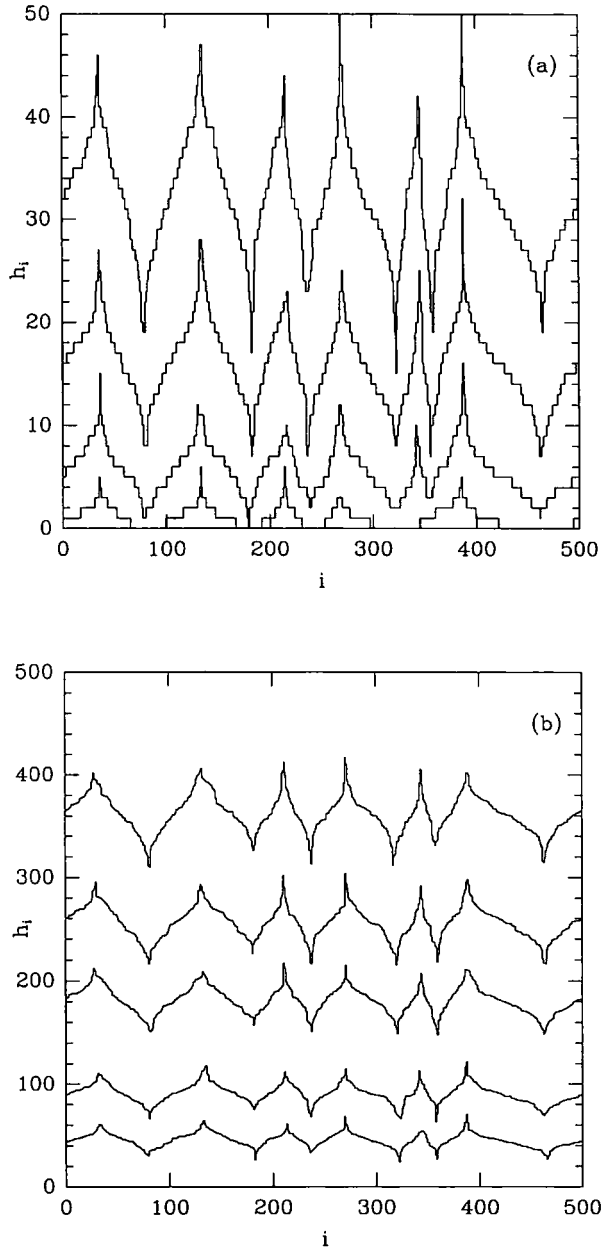

Fig. 1. Surface morphology for a system of 500 sites with $D/F = 5 \times 10^6$. Surface configurations after deposition of (a) (from bottom to top) 1, 5.6, 16, and 32 monolayers (ML), and (b) after 45.25, 90.5, 181, 256, and 362 ML. Note the different height scales in the two images.

the maxima of h_x form perfect barriers for the lateral mass transport. The same is true for the minima, due to the "Zeno effect" described by Elkinani and Villain:[13] Since only atoms which land at the level of the minimum contribute to the advancement of the adjoining steps, it takes a very long time for minima to close. These observations will become important in Section 3.

While the lateral structure is essentially frozen, the wedding cakes clearly steepen in the course of time. Figure 2 shows that the rescaling

$$h_x = \theta + \sqrt{\theta}\,\tilde{h}(x) \tag{3}$$

collapses the configurations at different times. This scaling is to be expected, since the variance of h_x is given by

$$W^2 = \langle (h_x - \theta)^2 \rangle = \theta \tag{4}$$

independent of D/F.[7] Here we are mainly concerned with characterizing the typical shape of $\tilde{h}(x)$ which is discernible in Fig. 2.

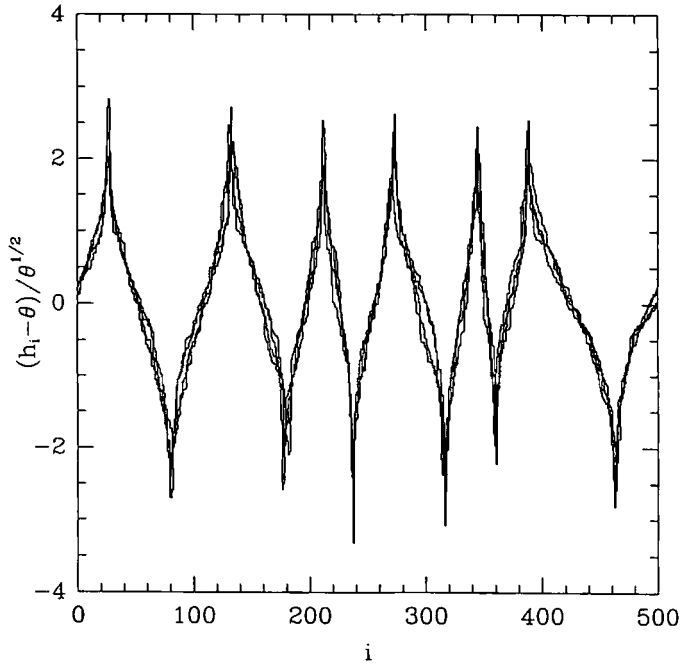

Fig. 2. Configurations after deposition of 1024, 2048, 4096, and 5792 ML, rescaled according to (3).

3. COVERAGE REPRESENTATION

The above discussion reveals two somewhat distinct sources of disorder in the growth process: one results from the irregularities in the spacings of the first layer nuclei, while the other is due to the shot noise during growth. To proceed, we eliminate the first source by focusing on half a wedding cake, i.e., the ascending hillside between a minimum and a maximum. We assume that no mass flux can pass the extrema, thus effectively placing the surface in a closed box of lateral size $L/2$ (Fig. 3). Moreover, we neglect the nucleation of new wedding cakes inside the box; since the morphology steepens, and consequently the terraces become shorter and shorter in the course of time, this is a reasonable approximation, though simulations show that occasionally new peaks can appear rather late in the growth process. The absence of nucleation implies that we let $D/F \to \infty$ inside the box, and the model parameter D/F enters only through the (externally imposed) length scale L.

After this sequence of approximations the surface has the shape of an ascending staircase which can be described by the set $\{l_h\}$ of (exposed) terrace lengths at height h (Fig. 3). For $D/F \to \infty$ the l_h have the dynamics of a noninteracting, fully asymmetric zero-range process.[6] In particular, the averages satisfy the linear equations

$$\frac{d}{d\theta}\langle l_h \rangle = \langle l_{h-1} \rangle - \langle l_h \rangle, \qquad h = 1, 2, 3, \ldots. \tag{5}$$

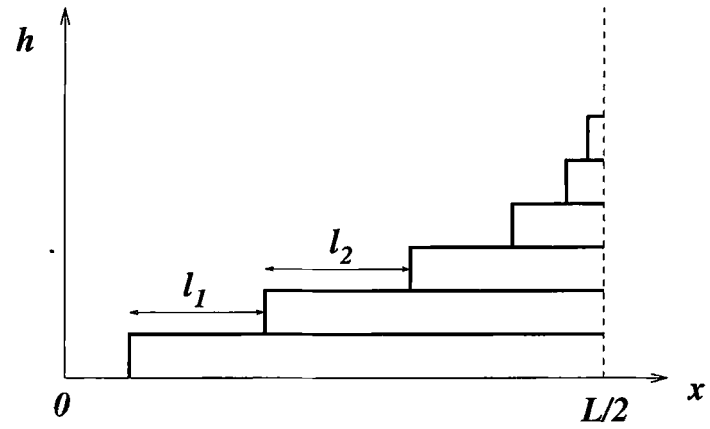

Fig. 3. Staircase geometry for half a wedding cake.

The bottom terrace (the exposed part of the substrate) evolves according to the Zeno equation[13]

$$\frac{d}{d\theta}\langle l_0\rangle = -\langle l_0\rangle \tag{6}$$

The solution with initial conditions $l_{h\geq 1}=0$ and $l_0=L/2$ is the Poisson distribution

$$\langle l_h\rangle = \frac{L}{2}\frac{e^{-\theta}\theta^h}{h!} \tag{7}$$

which for large coverages becomes a Gaussian,

$$\langle l_h\rangle = (L/2)(2\pi\theta)^{-1/2}\exp[-(h-\theta)^2/2\theta] \tag{8}$$

To transform this into the coarse-grained height profile $h(x,t)=\langle h_x(t)\rangle$ we merely note that the local terrace size is the inverse of the local slope,

$$\langle l_h\rangle = \partial x/\partial h \tag{9}$$

Integrating (8), we find the inverse height profile

$$x(h,t) = (L/4)(1+\mathrm{erf}(\Delta)) \tag{10}$$

where

$$\Delta = \frac{h-\theta}{\sqrt{2\theta}} \tag{11}$$

and

$$\mathrm{erf}(z) = (2/\sqrt{\pi})\int_0^z dy e^{-y^2} \tag{12}$$

Equation (10) confirms the scaling form (3) and identifies the scaling function for half a wedding cake as

$$\tilde{h}(x) = \sqrt{2}\,\mathrm{erf}^{-1}(4x/L-1) \tag{13}$$

Fig. 4 compares the asymptotic prediction with simulated wedding cakes; only the lateral size L has been fitted. The agreement is expected to improve for larger L, though presumably the relative fluctuations in the lateral spacing of wedding cakes (Fig. 1 and 2) will not decrease.

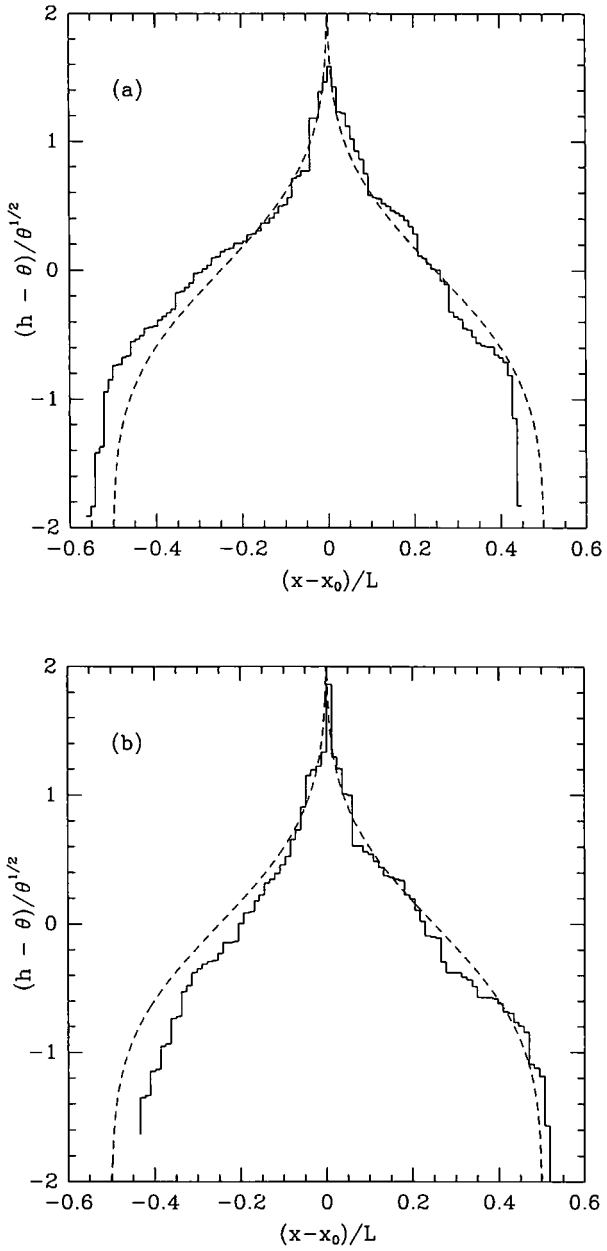

Fig. 4. Comparison of simulated wedding cakes (at 5792 ML) with the predicted asymptotic shape (dashed curve). The lateral distance L between minima has been fitted, and the shape has been shifted laterally to make the peaks coincide.

The shape is up–down symmetric under reflection at $h = \theta$; it will be seen in Section 5 that this is true only in one dimension. Moreover the height diverges, as $\tilde{h} \sim -\sqrt{\ln(1/x)}$, at the minima (and correspondingly at the maxima). Of course this divergence is cut off when the width of a groove or a peak becomes equal to the lattice spacing. This can be used to estimate the typical peak-to-valley height difference H—equivalently, the number of exposed layers—of the wedding cakes. Since (10) describes only half a wedding cake, the height of a minimum is obtained by setting $x(h) = 1/2$. Consequently

$$H = \sqrt{8\theta}\, \Delta_0(L) \tag{14}$$

where Δ_0 is the solution of

$$\Delta_0 \exp[\Delta_0^2] = \frac{L}{2\sqrt{\pi}} \tag{15}$$

which is a very slowly varying function of L.

These results are directly applicable to the experiments of Albrecht *et al.*[2] in which the formation of one-dimensional ridges with wedding-cake-like cross sections was observed during the homoepitaxy of Fe on Fe(110). Using low-energy electron diffraction (LEED), the evolution of the average terrace size $\bar{l}$ with coverage θ was monitored. At a growth temperature of 200 K it was found that $\bar{l}\sqrt{\theta}$ remained constant,[2] at about 10.7 atomic distances, for $1.9 \leqslant \theta \leqslant 9$. Since the wedding cake profile is monotonic between extrema, it follows that $\bar{l} = L/2H$, and using (14),

$$\bar{l}\sqrt{\theta} = \frac{L}{\sqrt{32}\, \Delta_0(L)} = \sqrt{\frac{\pi}{8}} \exp[\Delta_0^2] \tag{16}$$

Inserting the experimental value, one obtains $\Delta_0 \approx 1.68$, and from (15) the spacing of the ridges is estimated to be $L \approx 102$ atomic distances, about a factor of two larger than the estimate obtained by Albrecht *et al.* using a simpler, triangular model for the ridge shape; unfortunately, a direct measurement of L was not reported.

4. CONTINUUM LIMIT AND SINGULAR DIFFUSION

In this section it is shown how the shape function (13) can be derived directly from a continuum equation of motion for the growing surface

[2] The scaling $\bar{l} \sim 1/\sqrt{\theta}$ was also reported by Henzler[31] for two-dimensional wedding cakes on Ag(111).

$h(x, t)$. Such an equation has previously been proposed on heuristic grounds.[6, 14, 15] The argument can be explained using the configuration in Fig. 3: An atom landed on a terrace of size l moves, on average, a distance $l/2$ toward the ascending step edge, in the "uphill" direction. This implies a mass current $J = Fl/2 = (F/2)(\partial h/\partial x)^{-1}$ [compare to (9)]. The surface evolves through deposition and mass transport along the surface, hence

$$\frac{\partial h}{\partial t} = -\frac{\partial J}{\partial x} + F = -\frac{F}{2}\frac{\partial}{\partial x}\left(\frac{\partial h}{\partial x}\right)^{-1} + F \tag{17}$$

It is not clear that the argument remains valid in the regime $\partial h/\partial x > 1$ of primary interest here; we therefore provide a more careful derivation based on the exact equation (5) for the terrace lengths.

Let $l(h, t)$ denote the coarse-grained version of $\langle l_h(t) \rangle$. It is straightforward to derive an equation of motion for $l(h, t)$ starting from (5). First we introduce the Fourier transform

$$\hat{l}(q, t) = \sum_h e^{iqh} \langle l_h(t) \rangle \tag{18}$$

which satisfies

$$\partial \hat{l}/\partial \theta = (\exp(iq) - 1)\, \hat{l} \tag{19}$$

Coarse graining is accomplished by expanding $\exp(iq) - 1 \approx iq - q^2/2 + \mathcal{O}(q^3)$, and transforming back into real space, we have

$$\frac{\partial l}{\partial \theta} = -\frac{\partial l}{\partial h} + \frac{1}{2}\frac{\partial^2 l}{\partial h^2}. \tag{20}$$

Next we need to rewrite (20) in terms of $h(x, t)$ or, equivalently, in terms of the local slope $u(x, t) = \partial h/\partial x = 1/l$. This is achieved through a somewhat subtle manipulation[8] which has been referred to as a Lagrange transformation.[11] First we introduce $x(h, t)$, the inverse of $h(x, t)$. Evidently

$$\partial x/\partial h = l \tag{21}$$

Taking the time derivative of (21) and using (20), we further obtain

$$\partial x/\partial \theta = -l + (1/2)\, \partial l/\partial h \tag{22}$$

Now we can define an auxiliary function $\tilde{l}(x, t) = 1/u(x, t)$ through

$$l(h, t) = \tilde{l}(x(h, t), t) \tag{23}$$

Inserting (23) into (20) and using Eqs. (21) and (22), we find that several cancellations occur, and we are left with an autonomous equation for $\tilde{l}$,

$$\frac{\partial \tilde{l}}{\partial \theta} = \frac{1}{2} \tilde{l}^2 \frac{\partial^2 \tilde{l}}{\partial x^2} \tag{24}$$

In terms of $u(x, t) = 1/\tilde{l}(x, t)$ this becomes

$$\frac{\partial u}{\partial \theta} = -\frac{1}{2} \frac{\partial^2}{\partial x^2} \frac{1}{u} = \frac{1}{2} \frac{\partial}{\partial x} u^{-2} \frac{\partial u}{\partial x} \tag{25}$$

which is precisely the spatial derivative of (17).

Equation (25) has the form of a strongly singular diffusion equation with a diffusion coefficient diverging as u^{-2} for $u \to 0$. It was first studied [in the form (24)] by Rosen[8] in the context of heat conduction in solid H_2, who also observed that it can be linearized [into the form (20)] by following the reverse of the above procedure. Subsequently Bluman and Kumei[9] pointed out that the linearizability of the equation is related to the invariance under an infinite number of Lie–Bäcklund transformations; further results can be found in refs. 10 and 11. It is amusing to note that the simple growth model studied in this paper provides both a natural stochastic realization of the singular diffusion equation (25), and an intuitive interpretation of the linearizing transformation leading from (25) to (20).

It is now straightforward to verify that (13) can be obtained as a separable solution of the height equation (17). With the Ansatz

$$h(x, t) = \theta + A(t)\, g(x) \tag{26}$$

we find

$$2A\dot{A} = \frac{g''}{g(g')^2} = C > 0 \tag{27}$$

since $A, \dot{A} > 0$; here $\dot{A} = dA/d\theta$ and $g' = dg/dx$. We then observe that the differential equation for g is solved by setting

$$g' = \exp[(C/2)\, g^2] \tag{28}$$

The zero-current boundary conditions $J=(F/2)(Ag')^{-1}=0$ at $x=0$ and $x=L/2$ force g' and thus g to diverge at the boundaries. Consequently the integration constant C in (27) is fixed by

$$\int_{-\infty}^{\infty} dg(dx/dg)=\int_{-\infty}^{\infty} dg \exp[-(C/2)\, g^2]=L/2 \tag{29}$$

so that $C=8\pi/L^2$. Now (28) can be integrated, and yields

$$g(x)=(L/2\sqrt{\pi})\,\mathrm{erf}^{-1}(4x/L-1) \tag{30}$$

Finally the equation for A is integrated with initial condition $A(0)=0$, resulting in $A=\sqrt{8\pi\theta/L}$. The expression (26) for the height profile then reads

$$h(x,t)-\theta=\sqrt{2\theta}\,\mathrm{erf}^{-1}(4x/L-1) \tag{31}$$

in agreement with (13).

5. TWO DIMENSIONS

The extension of the minimal growth model to two dimensions is straightforward in principle; however, in order to obtain realistic island morphologies (see, e.g., refs. 1) it would be necessary to include some amount of edge diffusion (that is, diffusion of adatoms along island edges) and thus to give up the restriction that only singly bonded atoms can move.

We will not enter into these details here, but rather focus on one property of the one-dimensional model which carries over to the general case: Provided interlayer transport is completely suppressed, the differences between the coverages θ_h of two subsequent layers are given by a Poisson distribution,[7]

$$\theta_{h-1}-\theta_h=\frac{e^{-\theta}\theta^h}{h!} \tag{32}$$

in any dimension. This generalizes the result (7) for the one-dimensional case, where the coverage differences are proportional to the terrace lengths. For large values of the total coverage $\theta=\sum_h \theta_h$, (32) implies

$$\theta_h \approx (1/2)[1-\mathrm{erf}(\Delta)] \tag{33}$$

with Δ defined in (11).

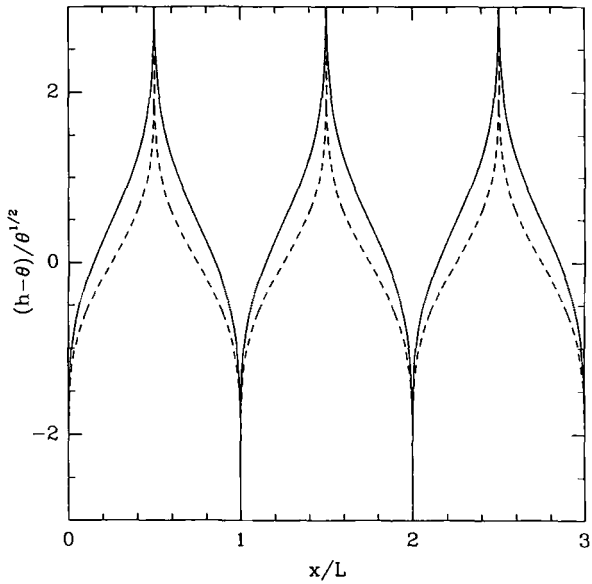

Fig. 5. Comparison of two-dimensional (full line) and one-dimensional (dashed line) shapes. The full line shows a cut through a square lattice array of wedding cakes with a square-shaped base.

Given that the coverages are known, the shape of the growing surface can be determined once a model for the mass distribution within one layer has been assumed. As a simple example, consider a square lattice array of square-shaped islands. If the distance between islands is L and the side length of an island in layer h is denoted by λ_h, the coverage is $\theta_h = (\lambda_h/L)^2$ and hence

$$\lambda_h \approx (L/\sqrt{2})[1 - \mathrm{erf}(\Delta)]^{1/2} \tag{34}$$

In Fig. 5 the resulting shape (for a cut along the axis of the square lattice array traversing the centers of the islands) is shown and compared to the one-dimensional case. The most important change is the loss of the up–down symmetry, which is simply due to the fact that the maxima are peaks, while the minima are (one-dimensional) grooves. On a more quantitative level one easily shows, using (34), that the typical height difference between a peak (H_+) or a groove (H_-) and the average height $h = \theta$ is given by

$$H_\pm \approx \sqrt{2\theta}\,\Delta_\pm \tag{35}$$

with

$$\Delta_+ \exp[\Delta_+^2] = \frac{L^2}{2\sqrt{\pi}} \tag{36}$$

and

$$\Delta_- \exp[\Delta_-^2] = \frac{L}{4\sqrt{\pi}} \tag{37}$$

For $L \to \infty$ the ratio $H_+/H_- \to \sqrt{2}$.

ACKNOWLEDGMENTS

I am most grateful to M. Schimschak for providing me with simulation data and to R. Ye for pointing out references to singular diffusion. This work was supported by DFG within SFB 237 Unordnung und grosse Fluktuationen.

REFERENCES

1. M. Bott, T. Michely, and G. Comsa, The homoepitaxial growth of Pt on Pt(111) studied with STM, *Surf. Sci.* **272**:161 (1992); J. Vrijmoeth, H. A. van der Vegt, J. A. Meyer, E. Vlieg, and R. J. Behm, Surfactant-induced layer-by-layer growth of Ag on Ag(111): Origins and side effects, *Phys. Rev. Lett.* **72**:3843 (1994); K. Bromann, H. Brune, H. Röder, and K. Kern, Interlayer mass transport in homoepitaxial and heteroepitaxial metal growth, *Phys. Rev. Lett.* **75**:677 (1995).
2. M. Albrecht, H. Fritzsche, and U. Gradmann, Kinetic facetting in homoepitaxy of Fe(110) on Fe(110), *Surf. Sci.* **294**:1 (1993).
3. M. Henzler, LEED from epitaxial surfaces, *Surf. Sci.* **298**:369 (1993).
4. J. Krug, Origins of scale invariance in growth processes, *Adv. Phys.* **46**:139 (1997).
5. G. Ehrlich and F. G. Hudda, Atomic view of surface self-diffusion: Tungsten on tungsten, *J. Chem. Phys.* **44**:1039 (1966); R. L. Schwoebel and E. J. Shipsey, Step motion on crystal surfaces, *J. Appl. Phys.* **37**:3682 (1966).
6. J. Krug and M. Schimschak, Metastability of step flow growth in $1+1$ dimensions, *J. Phys. France I* **5**:1065 (1995).
7. P. I. Cohen, G. S. Petrich, P. R. Pukite, G. J. Whaley, and A. S. Arrott, Birth–death models of epitaxy: I. Diffraction oscillations from low index surfaces, *Surf. Sci.* **216**:222 (1989).
8. G. Rosen, Nonlinear heat conduction in solid H_2, *Phys. Rev. B* **19**:2398 (1979).
9. G. Bluman and S. Kumei, On the remarkable nonlinear diffusion equation $(\partial/\partial x)[a(u+b)^{-2}(\partial u/\partial x)] - (\partial u/\partial t) = 0$. *J. Math Phys.* **21**:1019 (1980).
10. M. A. Herrero, A limit case in nonlinear diffusion, *Nonlinear Anal.* **13**:611 (1989); J. L. Vazquez, Nonexistence of solutions for nonlinear heat equations of fast-diffusion type, *J. Math. Pures Appl.* **71**:503 (1992).

11. P. Rosenau, Fast and superfast diffusion processes, *Phys. Rev. Lett.* **74**:1056 (1995).
12. J. Villain, A. Pimpinelli, L. Tang, and D. Wolf, Terrace sizes in molecular beam epitaxy, *J. Phys. I France* **2**:2107 (1992); A. Pimpinelli, J. Villain, and D. E. Wolf, Surface diffusion and island density, *Phys. Rev. Lett.* **69**:985 (1992).
13. I. Elkinani and J. Villain, Le paradoxe de Zenon d'Elee, *Solid State Commun.* **87**:105 (1993); Growth roughness and instabilities due to the Schwoebel effect: A one-dimensional model, *J. Phys. I. France* **4**:949 (1994).
14. J. Villain, Continuum models of crystal growth from atomic beams with and without desorption, *J. Phys. I France* **1**:19 (1991).
15. J. Krug, M. Plischke, and M. Siegert, Surface diffusion currents and the universality classes of growth, *Phys. Rev. Lett.* **70**:3271 (1993).